JOURNAL OF Applied Polymer SCIENCE

Optimization of Thermoelectric Properties of Metal-Oxide-Based Polymer Composites

Bastian Plochmann,[1] Steffen Lang,[2] Reinhold Rüger,[3] Ralf Moos[1]

[1]University of Bayreuth, Department of Functional Materials, Universitätsstraße 30, 95440 Bayreuth, Germany
[2]Siemens AG, CT RTC MAT POL-DE, Günther-Scharowsky-Str. 1, 91058 Erlangen, Germany
[3]Merck KGaA, PM-PFR-I, Frankfurter Str. 250, 64271 Darmstadt, Germany
Correspondence to: B. Plochmann (E-mail: bastian.plochmann@gmx.de)

ABSTRACT: Thermoelectric modules can be used for thermal energy harvesting. Common rigid thermoelectric stacks usually contain heavy metal alloys such as Bi_2Te_3. In order to substitute conventional materials and to reduce manufacturing costs, nontoxic, inexpensive and abundant materials using low-cost processes are first choice. This study deals with polymer composites consisting of a polysiloxane matrix filled with thermoelectric $Sn_{0.85}Sb_{0.15}O_2$ particles in micrometer scale. Thin composite sheets have been prepared by doctor blade technique and the Seebeck coefficient, the electrical and thermal conductivity, and the porosity were measured. Platelet-type particles, consisting of $Sn_{0.85}Sb_{0.15}O_2$-coated insulating mica substrate and globular $Sn_{0.85}Sb_{0.15}O_2$ particles have been varied in size, coating thickness and were mixed with each other in different ratios. The filler content was varied in order to maximize the figure of merit, ZT, to $1.9 \times 10^{-5} \pm 4 \times 10^{-6}$. Owing to their low raw material costs and the high degree of design freedom of polymer composites, one may use these materials in thermoelectric generators for remote low-power demanding applications. © 2013 Wiley Periodicals, Inc. J. Appl. Polym. Sci. **2014**, *131*, 40038.

KEYWORDS: conducting polymers; dyes/pigments; composites

Received 3 June 2013; accepted 4 October 2013
DOI: 10.1002/app.40038

INTRODUCTION

In order to convert waste heat from exhausts of combustion processes or in general from existing temperature gradients, for example, from a human body, directly into electricity, thermoelectric converters are under discussion.[1–4] For the latter case, biometric monitors and hearing devices are typical consumer applications.[3,4] Furthermore, instead of converting solar energy by photovoltaic cells, alternatively, thermoelectric generators can be used.[5,6]

Thermoelectric generators are abbreviated by TEG in the following. They base on the Seebeck effect. Even though the Seebeck effect has been known since 1821,[7] still today TEGs cannot be produced in a cost-effectively process, since the utilized raw materials like Bi_2Te_3 or Sb_2Te_3 are rather expensive and the production of devices is intricate.[3] In addition to that, the efficiency of TEGs is quite low.[2,5]

A measure for the thermoelectric efficiency is the figure of merit, ZT:

$$ZT = \frac{S^2\sigma}{\lambda} \cdot T \quad (1)$$

It depends on the squared Seebeck coefficient, S, the electrical conductivity, σ, the thermal conductivity, λ, and the absolute temperature, T.[8,9] The Seebeck coefficient is a materials constant, that depends on the charge carrier concentration, the effective density of states and the interaction of the charge carriers with the crystal lattice.[10]

On the materials side, today's research focuses on the substitution of expensive materials with low-cost skutterudites,[11] Half-Heusler alloys,[12] or doped metal oxides based on TiO_2,[13] SnO_2,[14] or donor-doped $SrTiO_3$,[15] with acceptable Seebeck coefficients and high electrical conductivities. By appropriate doping or thermal treatment, the charge carrier density, and therefore, the Seebeck coefficient can be tailored. As the electrical conductivity is proportional to the charge carrier density and the mobility of the charge carriers ZT reaches a maximum at medium charge carrier density.[16]

In order to further reduce costs, one tries to substitute rigid thermoelectric modules, which are typically ceramics-based stacks mounted as n- and p-type cubes, by new manufacturing approaches that include electrochemical processes[17] or by using flexible polymers as a mechanical basis of a TEG.[3,4,18] Polymeric materials for printed TEG-structures are also under investigation.[19]

Electrically insulating polymers, like epoxy resins, polysiloxanes, and polysilazanes become conductive by filling them with conductive particles. The electrical conductivity increases by orders of magnitude when the filler content reaches the percolation

threshold and approaches a saturation value with further increasing filler content. Both the saturation value and the percolation threshold depend on the applied materials, their morphology, and the size of the particles. Above the percolation threshold, conductive paths form a network of conducting particles in an insulating matrix. Their effective electrical conductivity depends mainly on the coulomb barriers between single particles.[20–22]

Filled polymers are, for example, in use to control the electrical potential of high-voltage generators.[23] They consist of a polymeric matrix like an epoxy resin filled with resistive metal oxide particles with a diameter of up to 10 μm and different aspect ratios.[23] The conductivity ranges from $\sigma = 10^{-11}$ to 10^{-8} Scm^{-1}. Other applications of filled polymers are printed circuit board tracks in electronic devices. They are characterized by highly conductive filler particles of silver or copper ($\sigma \approx 10^{4}$ Scm^{-1}) as well as by moderately conducting particles for antistatic applications like floors in exhibition halls ($\sigma \approx 10^{-4}$ Scm^{-1}).[20,24]

Conductive oxides, like stannic oxide, are typical n-type semiconductors for electronic applications.[25,26] They are also known as candidates for thermoelectric applications.[27] Therefore, in this study, tin-antimony-dioxide in a molar stoichiometry of $Sn_{0.85}Sb_{0.15}O_2$ was chosen as thermoelectric filler material.

Such thermoelectric composites enable to manufacture TEG modules with a large degree of design freedom. For instance, it has previously been described how a tubular TEG structure can easily be designed by flexible (semicured) polymeric and metallic strips as it is shown for instance in Ref. 28.

In order to optimize the figure of merit, *ZT*, of these composite materials, the present work investigates the manufacturing process and the performance optimization of composite layers for a TEG application. An insulating polysiloxane matrix, which is filled with thermoelectric $Sn_{0.85}Sb_{0.15}O_2$ filler particles, is applied by a doctor blade. The Seebeck coefficient, the thermal conductivity, and the electrical conductivity of the composites have been determined for different particle sizes, particle shapes, and particle filler ratios. The resulting porosity of the composite layers have been measured and compared to these thermoelectric parameters.

The aim of this investigation is to develop and characterize an inexpensive and nontoxic thermoelectric material, which can easily be manufactured by typical polymer manufacturing methods. It is NOT the intention of this work to achieve *ZT* values of commercial thermoelectric materials, but to open the path for flexible and very low-cost devices for energy harvesting for autonomously operating low-power devices.

EXPERIMENTAL

Base Materials and Fabrication

The particle diameter of the powder filler material is in the range of a few micrometers. Two different kinds of particle shapes are compared in this study: globular $Sn_{0.85}Sb_{0.15}O_2$ particles with a mean diameter of $d_g = 1$ and 10 μm, respectively, as well as platelet-like $Sn_{0.85}Sb_{0.15}O_2$ particles consisting of flat electrically insulating mica substrates with a functional $Sn_{0.85}Sb_{0.15}O_2$ surface coating. For coated particles, two types of insulating mica substrate were used—each with different mean particle diameters of $d_m = 7$ and 25 μm and thickness of $t_m = 220$ nm, respectively. This leads to huge contact areas between single particles in the composite. The polymers were applied by the doctor blade technique to align the particles by shear forces and to reduce interparticular electrical resistances at low filler contents.

A commercial polysiloxane matrix (Silres H62C, Wacker Chemie AG) was used to manufacture the composite materials. This polysiloxane matrix is state of the art for casting compound application.[29] It polymerizes at 200°C for 12 h by a polyaddition reaction. Polyadditional curing ensures that there is no volume shrinkage due to generation of volatile components during curing. All preparations were carried out at room temperature in ambient air. Toluene was used as a solvent to adjust the viscosity for filler contents between 25 and 50 vol %. For lower filler contents (15 and 20 vol %), fumed silica (1–5 wt %) was used to avoid sedimentation of the particles, which have a density of $\rho_{platelet} = 3.6$ gcm^{-1} and $\rho_{globular} = 6.5$ gcm^{-1}. The preparations were mixed up by a speed mixer (DAC 150 FVZ, Hauschild) at 3000 rpm for 15 s, until the dispersions became homogeneous. Afterwards, the preparations were applied by a 200-μm doctor blade on a separating foil (Pacothane, Pacothane Technologies) and dried in the fume hood for 12 h to slowly evaporate the solvent and to avoid blistering and cracking. Then, the samples were cured in the furnace, again at 200°C for 12 h. The homogeneity of the composite specimens was checked by optical microscopy.

Measurement Methods and Experimental Design

The composites were cut into strips of about 1–2 cm. Both ends of the specimens were coated with silver adhesive for low electrical contact resistances [Figure 1(a)]. The thickness of each layer, *t*, was measured with a micrometer gauge. The width, *w*, and resulting length, *l*, were determined with a caliper gauge. The electrical resistances, *R*, of the layers were measured with a multimeter (MM 7-1, Benning) or a "Megohmmeter" (M1501P, Sefelec) with a defined applied field of 1 Vmm^{-1}. The electrical conductivity of the composite, σ, was calculated using sample geometry and electrical resistance:

$$\sigma = \frac{1}{R} \cdot \frac{l}{w \cdot t} \tag{2}$$

The Seebeck coefficient, *S*, was determined by gluing the strips between two brass blocks using an electrically and thermally conductive silver adhesive. One of the brass blocks was positioned on a hotplate, the other one remained at room temperature [Figure 1(b)]. The distance between the hot and the cold side was about 1 cm. Thermocouples (type k) were located at the contact areas between sample and brass to measure the hot and the cold temperature, T_c and T_h, respectively. With the resulting Seebeck voltage, U_S, the Seebeck coefficient, *S*, was calculated by eq. (3):

$$S = \frac{U_S}{T_h - T_c} \tag{3}$$

After gluing the specimens on the brass blocks, the hotplate was heated up to 200°C, and afterward, it cooled down passively

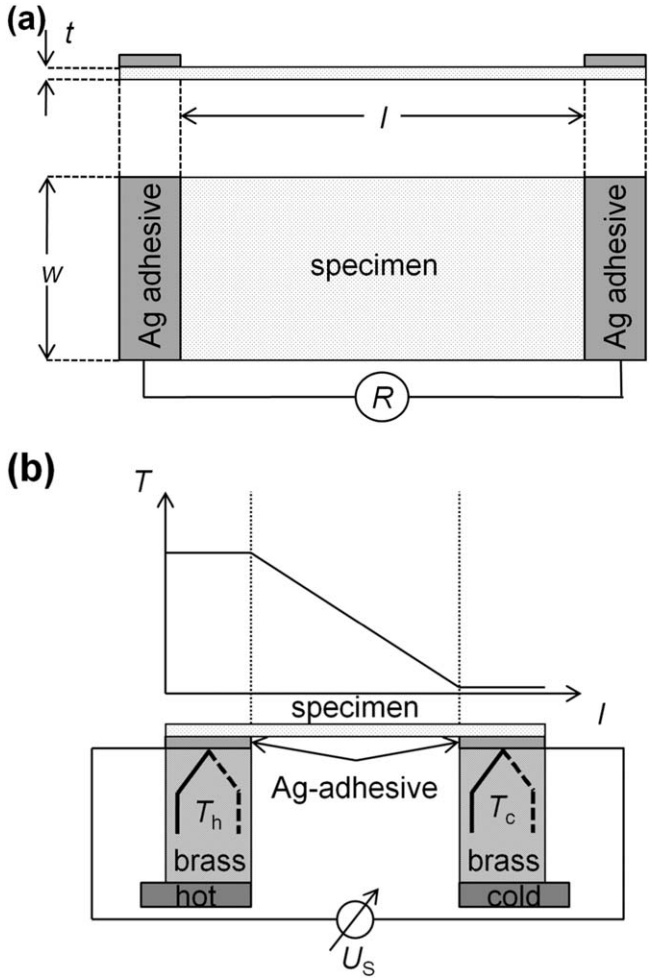

Figure 1. (a) Scheme of a thermoelectric composite sample with Ag adhesive for electrical characterization. (b) Test setup to determine the Seebeck coefficient: The TEG composite sample is clamped on two brass blocks, on which k-type thermocouples and a voltmeter are connected. One of the brass blocks is heated on a hotplate.

(heater off) in ~1 h to room temperature. During that procedure, a dataset of T_h, T_c, and U_S was recorded every 10 s and the Seebeck coefficient, $S(T)$, was calculated with T being the average of T_h and T_c. In principle, the Seebeck coefficient S is not determined correctly by eq. (3), since the thermopower of brass is not considered.[30] However, its value of $-0.49\ \mu VK^{-1}$ at room temperature ($T = 300$ K) and $-0.13\ \mu VK^{-1}$ at 450 K can be neglected compared to the Seebeck coefficient of $Sn_{0.85}Sb_{0.15}O_2$.

The thermal diffusivity, α, of the thermoelectric composite foils was measured with Laser Flash Analysis (LFA 447, Netzsch). The thermal diffusivity is highly anisotropic due to the anisotropic filler material geometry, but only the in-plane thermal diffusivity is of interest for the application. Therefore, 80 little strips were cut out of one sample, rotated by 90° and stacked together. The direction of the aligned platelet-type particles in the resulting quadratic specimen is now cross-plane. The strips were glued together with epoxy adhesive with special care not to generate bonding gaps, which could distort the measurements. Afterward, the samples were trimmed and deflashed to fit for the LFA specimen holder.

Table I. Matrix of Prepared Samples and Type of Conducted Measurement

Filler content/vol %	Volumetric ratio of globular : platelet particles				
	100 : 0	75 : 25	50 : 50	25 : 75	0 : 100
15	σ, p, λ	σ, p	σ, p	σ, p	σ, p
20	σ, p, S, λ	σ, p	σ, p	σ, p	σ, p, S
25	σ, p, S, λ	σ, p	σ, p	σ, p	σ, p, S
30	σ, p, S, λ	σ, p, S, λ	σ, p, S, λ	σ, p, S, λ	σ, p, S, λ
40	σ, p, S, λ	σ, p	σ, p	σ, p	σ, p, S
50	σ, p, S, λ	σ, p	σ, p	σ, p	σ, p, S

The filler content was varied from 15 to 50 vol %, the mixture ratio of platelet-type and globular particles was varied in 25-vol % steps.

The specific heat capacity, c_p, was measured by dynamic scanning calorimetry (Q100 DSC, TA Instruments) and the density, ρ, was determined by the method of Archimedes. The porosity in percentage, p, can be determined from the measured density, ρ, and the density of the composite material, ρ_0, as calculated from the densities of filler and polymeric material:

$$p = \left(1 - \frac{\rho}{\rho_0}\right) \cdot 100\% \tag{4}$$

The thermal conductivity, λ, can be calculated from the above-determined variables as[31]:

$$\lambda = \alpha \cdot \rho \cdot c_p \tag{5}$$

Table I gives an overview over all measured parameters at different filler mixtures and filler contents.

The electrical conductivity, σ, and the porosity, p, were measured for six different filler contents in the polysiloxane matrix: 15, 20, 25, 30, 40, and 50 vol %. For each of these six filler content levels, two types of particles were admixed in five different samples.

Figure 2(a) shows schematically the structure of both kinds of particles. The first kind are platelet-like particles consisting of a mica substrate (thickness mica $t_m = 220$ nm, diameter mica $d_m = 7\ \mu$m) coated with a $Sn_{0.85}Sb_{0.15}O_2$ layer (coating thickness $t_c = 25$ nm). Figure 2(b) shows an SEM image of these coated platelet-type particles. The second kind of particles are globular $Sn_{0.85}Sb_{0.15}O_2$ particles without substrate (diameter $d_g = 1\ \mu$m). Figure 2(c) shows an SEM image of the globular particles. Platelet-type and globular-type particles were mixed in volumetric ratios of 100 : 0, 75 : 25, 50 : 50, 25 : 75, and 0 : 100.

Due to the thin samples (uncertainty of micrometer gauge) and the electrical contact resistances the uncertainty is estimated to be $\Delta_\sigma = 5\%$. In order to calculate ZT for all particle mixtures and filler content variations, the Seebeck coefficient was measured for all samples with volumetric ratios of 100 : 0 and 0 : 100 for a filler content of 20–50 vol %, as well as for the mixed particle samples at a filler content of 30 vol %. It was estimated that the Seebeck coefficient is independent of the filler content;

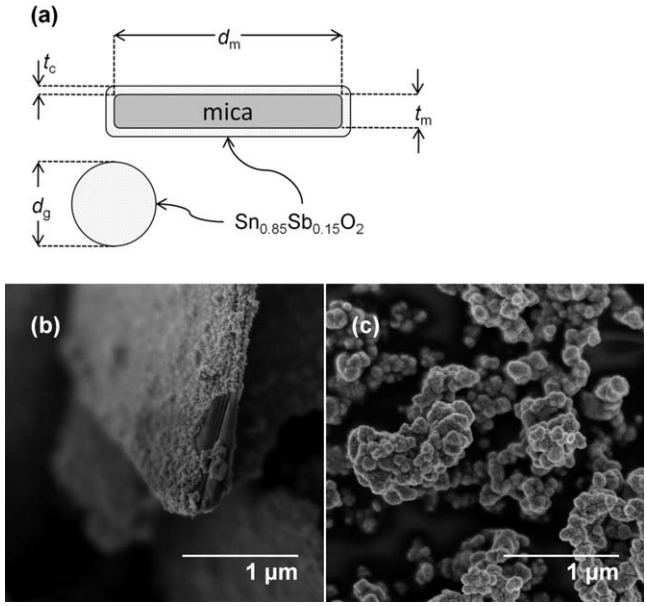

Figure 2. (a) Scheme of $Sn_{0.85}Sb_{0.15}O_2$ filler particle types: coated platelet-type particles with mica substrate and globular particles without substrate. (b) SEM image of a $Sn_{0.85}Sb_{0.15}O_2$-coated mica substrate. (c) SEM image of globular $Sn_{0.85}Sb_{0.15}O_2$ particles without substrate.

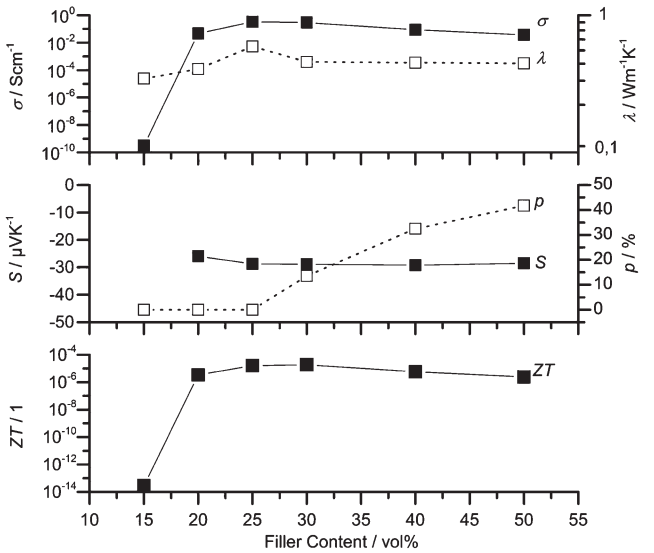

Figure 3. Electrical conductivity, σ, thermal conductivity, λ, Seebeck coefficient, S, porosity, p, and figure of merit, ZT, of globular particles in a polysiloxane matrix in dependence of the filler content between 15 and 50 vol %.

therefore, the measured Seebeck coefficients at 30 vol % were used for all filler contents. The measurement uncertainty for S is estimated to be ±10%, as a result of thermal and electrical contact resistances in the measurement setup and the uncertainty of the thermocouples (±1%). The thermal conductivity, λ, was measured for all samples with volumetric ratio 100 : 0 and additionally for a filler content of 30 vol % for the ratios 75 : 25, 50 : 50, 25 : 75, and 0 : 100, respectively. The slope of λ at different filler contents at a particle ratio of 100 : 0 was used to extrapolate the values of the remaining particle ratios. The uncertainty of the thermal diffusivity is 3% according to the manufacturer. Due to the thin composite samples, the uncertainty of the calculated λ is estimated to be ±5%. For all samples, ZT was calculated from the measured and determined values according to eq. (1). The uncertainty of ZT, $\Delta_{ZT} = 21\%$, was calculated by Gaussian error propagation out of $\Delta_\sigma = 5\%$, $\Delta_\lambda = 5\%$, and $\Delta_S = 10\%$.

The composites that consist of pure platelet particles were further investigated with respect to their electrical conductivity, by using particles with larger mica substrate diameters, $d_m = 25$ µm, and varying the $Sn_{0.85}Sb_{0.15}O_2$ coating thickness ($t_c = 25$, 50, 80, and 120 nm). The filler content of the polymer matrix of these samples was 30 vol %. The globular particle composites were further investigated concerning σ, p, S, and λ with bigger particles ($d_g = 10$ µm) and mixing them with the previously used smaller particles ($d_g = 1$ µm) in the volumetric ratios of 100 : 0, 75 : 25, 50 : 50, 25 : 75, and 0 : 100, respectively. These composite samples contain 50 vol % filler content in the polymer matrix.

RESULTS AND DISCUSSION

All measurements for σ, λ, and p were carried out at room temperature. The presented Seebeck coefficients were determined at a temperature of 50°C. The temperature dependence of these four parameters is low and can therefore be neglected in the range between 20 and 50°C.

Particle Shape Mixtures and Filler Content Variation

Figure 3 shows the parameters σ, λ, S, and p versus the filler contents of globular particles in the polysiloxane matrix. The figure of merit, ZT, which is computed concerning eq. (1) is shown in this figure, too.

For a filler content of 15 vol %, the conductivity $\sigma_{15,100} = 3 \times 10^{-10}$ Scm^{-1} is quite low but increases abruptly with a maximum of $\sigma = 3.3 \times 10^{-1}$ Scm^{-1} at 25 vol % and decreases (slightly in the logarithmic scale) for even higher filler contents. The sudden increase can be explained by percolation paths that begin to form above a defined volume content of conductive particles. Then, the samples become conductive with a slightly increasing conductivity, a well-known phenomenon for polymer metal or carbon mixtures.[32,33] Above a filler content of 30%, the porosity increases, which is due to the evaporation of toluene in conjunction with the low viscosity of the highly filled matrix. As a result of the increasing porosity, above a filler content of 30 vol % the conductivity decreases again a little.

The thermal conductivity of the sample with a filler content of 15 vol % ($\lambda = 0.35$ $Wm^{-1}K^{-1}$) is already a bit higher than the thermal conductivity of pure polysiloxane with $\lambda \approx 0.2$ $Wm^{-1}K^{-1}$. It increases to 0.59 $Wm^{-1}K^{-1}$ and remains almost constant not depending of the amount of added filler.

The Seebeck coefficient of the almost insulating sample at 15 vol % could not be measured. This is a well-known and often-observed phenomenon when measuring Seebeck coefficients, since it is difficult to measure small voltages on high-ohmic sources.[34,35] As soon as the percolation threshold is reached, the Seebeck coefficient could be measured. It is between $S = -26$ μVK^{-1} and $S = -30$ μVK^{-1}. Such filler-independent behavior

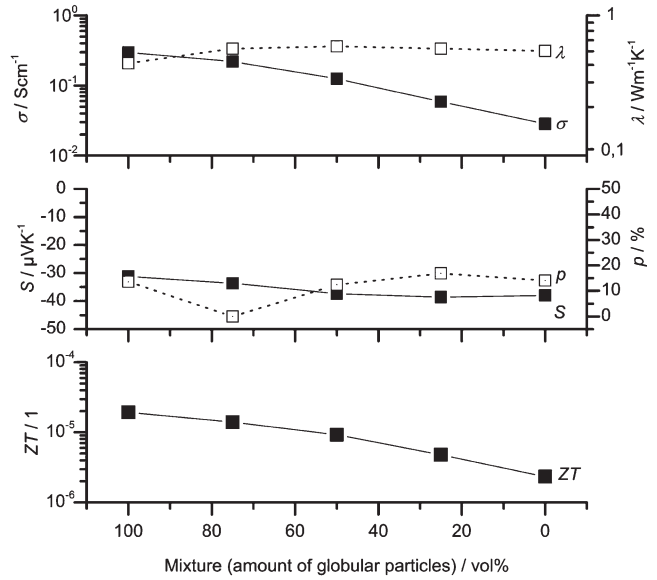

Figure 4. Electrical conductivity, σ, thermal conductivity, λ, Seebeck coefficient, S, porosity, p, and figure of merit, ZT, of mixtures between globular and platelet-type particles in a polysiloxane matrix at a filler content of 30 vol %.

was expected because the Seebeck coefficient is a materials property that is defined by a potential difference and a temperature difference.[36] Hence, it does not matter, whether one determines the voltage between two points of a homogenous film of the material, or of a porous system, or even of small paths.[37]

The figure of merit, ZT, is calculated according to eq. (1). Its behavior mirrors the conductivity. It reaches a maximum of 1.7×10^{-5} to 1.9×10^{-5} for filler contents between 25 and 30 vol %. Obviously for globular particles, a filler content of about 30 vol % yields the highest figure of merit. For that purpose, the following mixture experiments with globular and platelet particles were conducted with a filler content of 30 vol %.

Figure 4 shows the results. All specimens in Figure 4 consist of 30 vol % filler content. The electrical conductivity decreases the higher the amount of platelet particles is. As the Seebeck coefficient, the porosity, and the thermal conductivity remain almost constant, the figure of merit behaves again like the conductivity. It decreases by about one order of magnitude from $ZT = 1.9 \times 10^{-5}$ for pure globular particles to $ZT = 2.3 \times 10^{-6}$ for pure platelet-filler mixtures.

For the sake of completeness, the entire set of filler contents as depicted in Table I was investigated. Figure 5 shows a three-dimensional graph of the calculated figure of merit, ZT, according to eq. (1). The filler content was varied from 15 to 50 vol % and the particle type mixtures were varied in 25% steps analogously to Figure 4. The maximum figure of merit, $ZT_{30,100} = (1.9 \pm 0.4) \times 10^{-5}$, can be found at a filler content of 30 vol % and a volumetric ratio of 100 : 0, that is, for purely globular particles.

It becomes obvious that for these composite materials, ZT is dominated by the electrical conductivity because σ varies by orders of magnitude with the filler content and the particle type. The thermal conductivity varies only by factor of 2. Furthermore, the Seebeck coefficients remain constant at different filler contents (since the charge carrier density in the particles remains constant). The Seebeck coefficient is independent of the filler content as long as a conductive percolating network exists in the composite material (above the percolation threshold). Different filler contents in a polymeric matrix can be

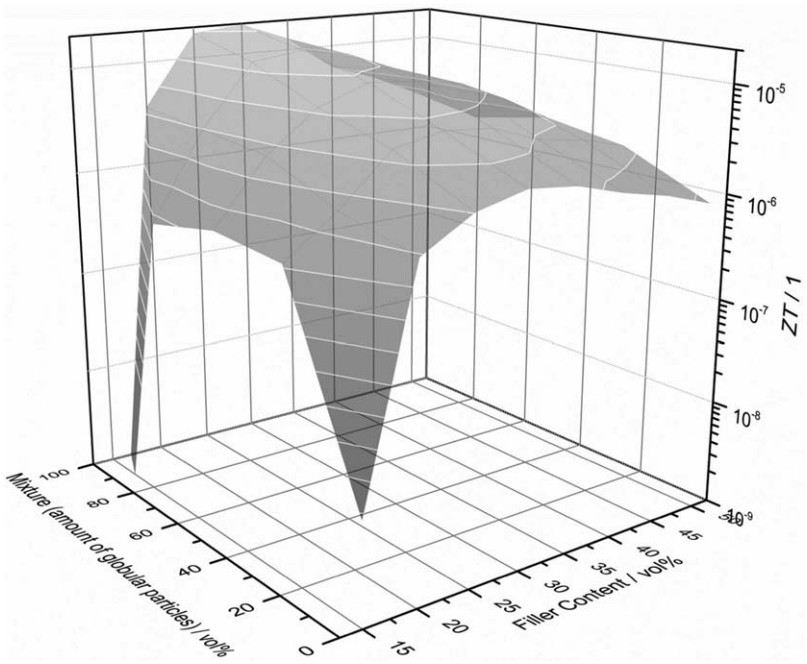

Figure 5. Figure of merit, ZT, of particle mixtures in a polysiloxane matrix at filler contents between 15 and 50 vol %. ZT is calculated acc. to eq. (1).

interpreted as different numbers of parallel conductive pathways "diluted" by the insulating polymer matrix. The decrease of both conductivities, σ and λ, is obviously correlated with the increasing porosity of the composite materials. For λ this is not surprising, since porous polymers are typically used for thermal insulation applications.[38] In case of σ, a slight negative slope could be explained by a decreasing conductor cross section in the composite material because of the presence of insulating pores. The disproportional decrease of σ of nearly one order of magnitude is perhaps due to broader gaps between the particles and therefore disconnected pathways in the percolating network. As a conclusion, one may state that an increasing porosity in the polymer composite yields a decreasing figure of merit.

In case of low filler contents (15–20 vol %) aligned platelet-like particles provide a stable electrical conductivity at low filler contents in contrast to globular-like particles due to the shifted percolation threshold.[20] Composites with mixtures of globular-like and platelet-like particles improve the electrical conductivity of the polymer composite at low filler contents by two orders of magnitude. This effect is again caused by a percolation threshold further shifted to lower filler contents by using a mixture of platelet-type and globular particles.[20] Therefore, it may be possible to achieve acceptable conductivities at filler contents below 15 vol %. For higher filler contents (25 to 30 vol %), the platelet substrates do not show higher electrical conductivities. Globular particles with low intrinsic resistances lead to the highest electrical conductivities between 3.3×10^{-1} and 2.8×10^{-1} Scm^{-1}, respectively, and therefore to the highest figure of merit, with $ZT = (1.9 \pm 0.4) \times 10^{-5}$. As a conclusion, it must be additionally emphasized that globular particles do not lead to an anisotropic polymer composite in contrast to aligned platelet-like particles.

The achieved figure of merit of 1.9×10^{-5} is low in contrast to conventional inorganic thermoelectric materials reaching a figure of merit of almost 1, but it reaches the ZT range of current polymeric solutions between 10^{-5} and 0.25.[37] For a specific application, material and processing costs need to be weighted up against the figure of merit and efficiency of the TEG. Metal oxide particles and polysiloxanes are extremely inexpensive commercial mass products and therefore ready for a cost-efficient industrial use.

Improving the Properties of the Platelet-Type Particles

In order to improve the electrical conductivity of the polymer composites containing coated platelet-like particles, it is obvious to enlarge the diameter of the mica substrates, d_m. By simultaneously maximizing the coating layers on these optimized substrates, a greater volumetric ratio of insulating substrate material and thermoelectric $Sn_{0.85}Sb_{0.15}O_2$ can be obtained.

Figure 6 shows the electrical conductivity of composite materials consisting of platelet-type particles with a substrate diameter $d_m = 7$ μm and a substrate thickness $t_m = 220$ nm as well as $d_m = 25$ μm and $t_m = 220$ nm, respectively. The substrate is coated with a $Sn_{0.85}Sb_{0.15}O_2$ functional layer. The coating thickness is varied from $t_c = 25$–120 nm. The matrix material is the same polysiloxane (Silres H62C, Wacker Chemie AG) as in the previous test series. A filler content of 30 vol % was chosen. As expected, the increase in the functional coating layer thickness yields a slightly higher conductivity. However, this behavior occurs only for $t_c = 50$ nm. Much lower conductivities are found for $t_c = 80$ nm and $t_c = 120$ nm. This is astonishing at first glance. One would have expected an increasing conductivity with increasing coating layer thickness. However, figure 7 helps to explain this behavior. The SEM images of these filler materials show completely faultless functional coating layers in Figure 7(a) ($t_c = 25$ nm) and Figure 7(b) ($t_c = 50$ nm) with some particles on the surface. In Figure 7(c), one finds first

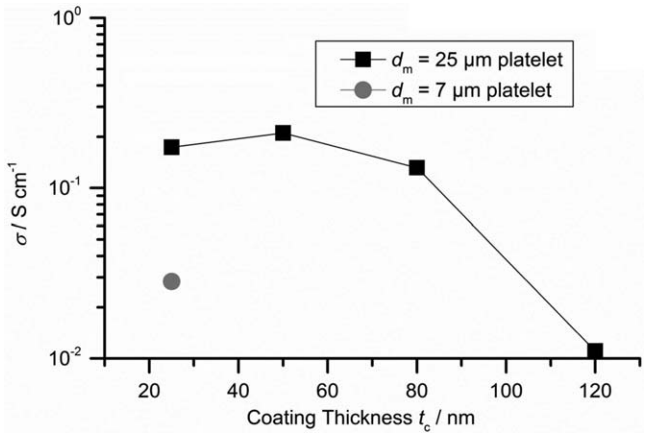

Figure 6. Electrical conductivity, s, of coated substrate particles with different functional layer thicknesses ($t_c = 25$, 50, 80, and 120 nm). The filler content is 30 vol % in a polysiloxane matrix.

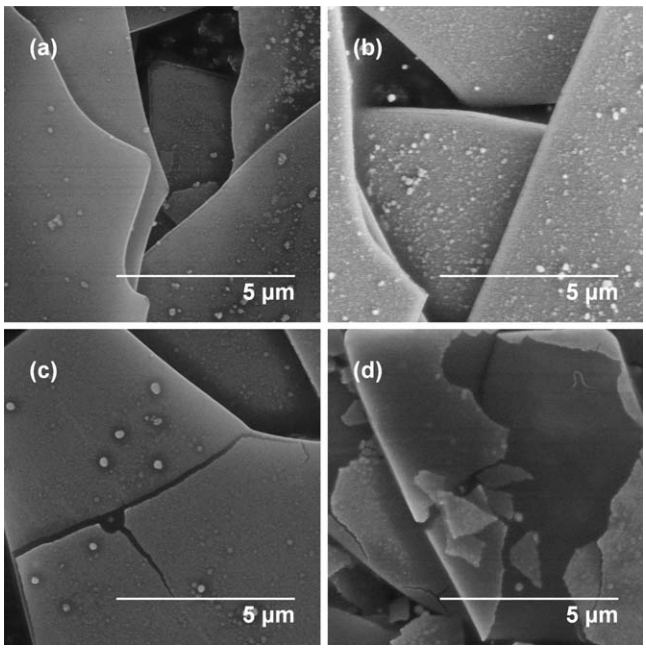

Figure 7. SEM images of platelet-type particles with different coating layer thicknesses t_c. (a) $t_c = 25$ nm. The coating layer is crack-free (b) $t_c = 50$ nm. The coating layer shows some particles at the surface. (c) $t_c = 80$ nm. Cracks appear on the coating layer. (d) $t_c = 120$ nm. The coating layer is cracked and delaminated.

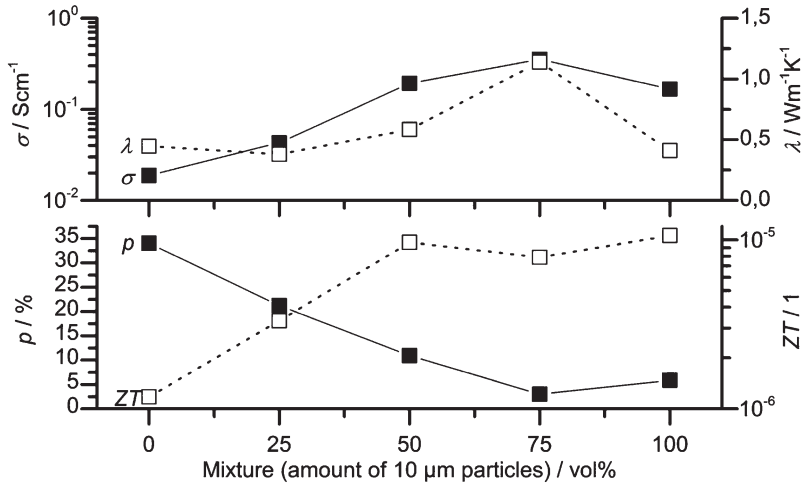

Figure 8. Electrical conductivity, σ, thermal conductivity, λ, porosity, p, and figure of merit, ZT, of $d_g = 10$ μm and $d_g = 1$ μm globular particle mixtures. The samples consist of 50-vol % filler content in a polysiloxane matrix.

cracks growing in the surface coating and Figure 7(d) shows that the functional coating layer is flaking off the substrate. Therefore, it is assumed that by reaching a certain coating-thickness, the functional layer cracks and flakes off the substrate, yielding a lower conductivity.

The electrical conductivity of the sample with the particle parameters $t_c = 25$ nm, $d_m = 25$ μm, and $t_m = 220$ nm is six times higher than the conductivity of the sample with the smaller particle diameter of only $d_m = 7$ μm. The conductivity increase with greater substrate diameters, d_m, could be caused by fewer contact points between particles in the composite materials in plane direction. Nevertheless, the cross plane conductivity is decreasing with greater substrate diameters, d_m, and therefore, the anisotropy rises.

Improving the Globular Particles

In order to further increase the figure of merit of the composite samples, globular-like $Sn_{0.85}Sb_{0.15}O_2$ particles with a diameter $d_g = 10$ μm were mixed with globular particles with $d_g = 1$ μm. Different volumetric filler particle ratios in the polysiloxane matrix were studied. The polysiloxane matrix (H62C, Wacker Chemie AG) was filled with volumetric filler ratios of 0 : 100, 25 : 75, 50 : 50, 75 : 25, and 100 : 0 ($d_g = 1$ μm : $d_g = 10$ μm), respectively.

Figure 8 shows data of the electrical and the thermal conductivity, of the porosity, and of the calculated figure of merit, ZT. The Seebeck coefficient, $S = -29$ μVK^{-1}, was not found to vary significantly in these mixtures. With a higher volume content of large particles ($d_g = 10$ μm), the porosity decreases to a minimum of 3% at a volumetric ratio of 75 : 25. The electrical conductivity and the thermal conductivity behave inversely to the porosity and reach maximum values for the same particle mixture ratio: 0.35 Scm^{-1} and 1.14 $Wm^{-1}K^{-1}$, respectively. The figure of merit increases with a higher amount of large particles and lower porosity, but no outstanding maximum appears. Between the ratios 50 and 100 vol % of large particles, its value remains more or less the same: $ZT = 1.0 \times 10^{-5}$, due to the similar behavior of thermal and electrical conductivity.

It is known that maximum packing density of a monomodal particle distribution is 64 vol %.[39] This maximum shifts to higher possible densities by using an ideal bimodal or even higher modal particle distribution. Therefore, the viscosity of a sample preparation with a bimodal particle distribution is lower than a monomodal one of the same filler content.[39] For practical application, this means that less toluene is needed to control the viscosity of the preparations. Accordingly, the porosity of the cured composites decreased as well.

CONCLUSIONS

In summary, we find that the electrical and thermal conductivity of thermoelectric composite materials depend on shape and size of the filler particles as well as on filler content and porosity of the polysiloxane matrix. For lower filler contents, a mixture of platelet-type and globular particles shows a significantly better conductivity than pure globular particles. In the filler content range between 20 and 30 vol %, the small intrinsic resistivity of the globular particles without an insulating substrate overbalances the good particle connections of aligned platelets. Therefore, pure globular particles offer the highest conductivity at 25–30 vol % filler content of about 3×10^{-1} Scm^{-1} as well as the highest figure of merit, of 1.9×10^{-5}. In addition, globular particles offer no anisotropy like aligned platelet particles, providing much more possibilities for application and usage. Higher filler contents, 40 and 50 vol %, cause a high porosity of the composite layers, due to low fabricating viscosities and therefore a higher demand for toluene. This porosity reduces the electrical as well as the thermal conductivity and leads to a figure of merit decrease by about one order of magnitude. Therefore, porosity is not beneficial for this polymeric thermoelectric solution. The use of other lower viscous matrices, for example, epoxy resins, could offer a smaller porosity due to the minor demand for a solvent.

Using platelet-like substrates with a greater diameter and a smaller thickness leads to better in-plane electrical conductivity. However, the anisotropic behavior rises as well. By increasing the functional coating layer thickness on the platelet substrate, from 25 to 120 nm, the electrical conductivity does not increase significantly. The reason is that functional coating layer cracks and flakes off at higher thicknesses.

The maximum figure of merit of 1.9×10^{-5} reveals a potential for applications as TEG in energy harvesting low power demanding sensor systems. The huge advantage compared to conventional materials is the high degree of design freedom of polymers combined with the extremely low cost compared to conventional TEG materials. All further improvements to increase the figure merit need to deal with very inexpensive, nontoxic and abundant raw materials as matrix materials for the polymers.

Further investigations in thermoelectric composites are suggested in the area of bimodal or higher modal fraction distributions for maximizing the electrical conductivity and minimizing the porosity at high filler contents. Furthermore, alternative polymer processing routes like extrusion or casting may lead to high filler contents without the need for a solvent and consequently lower porosity.

ACKNOWLEDGMENTS

We gratefully acknowledge the mentoring of the Projektträger Jülich (PtJ) as well as the financial support of the Bundesministerium für Bildung und Forschung (BMBF).

REFERENCES

1. Weilguni, M.; Franz, M.; Slyusar, N. Feasibility Study and Life Cycle Energy Balance of Thermoelectric Generator Modules for Automotive Applications, *35th International Spring Seminar on Electronics Technology*; Bad Aussee, Austria, **2012**, p 355.
2. Qiu, K.; Hayden, A. C. S. *J. Electron. Mater.* **2009**, *38*, 1315.
3. Francioso, L.; De Pascali, C.; Farella, I.; Martucci, C.; Cretì, P.; Siciliano, P.; Perrone, A. *J. Power Sources* **2011**, *196*, 3239.
4. Weber, J.; Potjekamloth, K.; Haase, F.; Detemple, P.; Volklein, F.; Doll, T. *Sens. Actuators A* **2006**, *132*, 325.
5. McEnaney, K.; Kraemer, D.; Ren, Z.; Chen, G. *J. Appl. Phys.* **2011**, *110*, 074502.
6. Li, P.; Cai, L.; Zhai, P.; Tang, X.; Zhang, Q.; Niino, M. *J. Electron. Mater.* **2010**, *39*, 1522.
7. Carmo, J. *IEEE Trans. Ind. Electron.* **2010**, *57*, 861.
8. Jalan, B.; Stemmer, S. *Appl. Phys. Lett.* **2010**, *97*, 042106.
9. Tritt, T.; Böttner, H.; Chen, L. *MRS Bull.* **2008**, *33*, 366.
10. Rettig, F.; Moos, R. *Sens. Actuators B* **2010**, *145*, 685.
11. Yang, J.; Hao, Q.; Wang, H.; Lan, Y.; He, Q.; Minnich, A.; Wang, D.; Harriman, J.; Varki, V.; Dresselhaus, M.; Chen, G.; Ren, Z. *Phys. Rev. B* **2009**, *80*, 115329.
12. Joshi, G.; Yan, X.; Wang, H.; Liu, W.; Chen, G.; Ren, Z. *Adv. Energy Mater.* **2011**, *1*, 643.
13. Tang, J.; Wang, W.; Zhao, G.-L.; Li, Q. *J. Phys.: Condens. Matter* **2009**, *21*, 205703.
14. Yanagiya, S.; Nong, N. V.; Xu, J.; Sonne, M.; Pryds, N. *J. Electron. Mater.* **2011**, *40*, 674.
15. Moos, R.; Gnudi, A.; Härdtl, K. H. *J. Appl. Phys.* **2005**, *78*, 5042.
16. Mahan, G. D. *J. Appl. Phys.* **1989**, *65*, 1578.
17. Schwyter, E.; Glatz, W. Flexible micro thermoelectric generator based on electroplated $Bi_{2+x}Te3$-x. In *DTIP, Nice*, **2008**.
18. Hasebe, S.; Ogawa, J. Polymer based smart flexible thermopile for power generation. In *17th IEEE International Conference on Micro Electro Mechanical Systems*; Maastricht, The Netherlands, **2004**; p 689.
19. Madan, D.; Chen, A.; Wright, P. K.; Evans, J. W. *J. Appl. Phys.* **2011**, *109*, 034904.
20. Pfaff, G.; Kuntz, M.; Rüger, R. Electro-conductive pigments for coating application; In *8th International Conference ACT'08*; Warschau, **2008**; p 117.
21. Kishimoto, A.; Takagawa, Y.; Teranishi, T.; Hayashi, H. *Mater. Lett.* **2011**, *65*, 2197.
22. Yi, Y. B.; Esmail, K. *J. Appl. Phys.* **2012**, *111*, 124903.
23. Lang, S. Höchstleistungswerkstoffe für energieeffiziente Generatoren durch Einsatz innovativer Endenglimmschutzsysteme (in German), *Dissertation, University of Erlangen-Nürnberg*, **2013**.
24. Ott, F.; Patzlaff, J.; Rüger, R. *PPCJ* **2006**, 28.
25. Dakhel, A. A. *Sol. Energy* **2012**, *86*, 126.
26. Woo, D. C.; Koo, C. Y.; Ma, H. C.; Lee, H. Y. *Trans. Electr. Electron. Mater.* **2012**, *13*, 241.
27. Yanagiya, S.; Nong, N. V.; Xu, J.; Sonne, M.; Pryds, N. *J. Electron. Mater.* **2011**, *40*, 674.
28. Plochmann, B.; Lang, S. Thermoelektrisches Generatorrohr und Verfahren zur Herstellung des Generatorrohrs, *German Patent Application* DE 10 2012 208 225, (**2012**).
29. Wacker AG, Technical Data Sheet V 1.5 Silres® H62C 2013, (http://www.wacker.com).
30. Rosenfeld, A. M.; Timsit, R. S. *Philos. Mag. Part B* **1984**, *49*, 111.
31. Alboni, P. N.; Ji, X.; He, J.; Gothard, N.; Hubbard, J.; Tritt, T. M. *J. Electron. Mater.* **2007**, *36*, 711.
32. Stankovich, S.; Dikin, D.; Dommett, G.; Kohlhaas, K.; Zimney, E.; Stach, E.; Piner, R.; Nguyen, S.; Ruoff, R. *Nature* **2006**, *442*, 282.
33. McQueen, D.; Jäger, K.; Paligova, M. *Macromol. Symp.* **2005**, *221*, 217.
34. Rettig, F.; Moos, R. *Meas. Sci. Technol.* **2009**, *20*, 065205.
35. Rettig, F.; Moos, R. *Sens. Actuators B* **2007**, *123*, 413.
36. Rettig, F.; Moos, R. *IEEE Sensors J.* **2007**, *7*, 1490.
37. Stöcker, T.; Köhler, A.; Moos, R. *J. Polym. Sci. Part B: Polym. Phys.* **2012**, *50*, 976.
38. Kim, J.; Lee, J.-H.; Song, T.-H. *Int. J. Heat Mass Transfer* **2012**, *55*, 5343.
39. Uebler, M. Verbesserung bruch—und (thermo)mechanischer Eigenschaftskennwerte mikroskalig—gefüllter Epoxidharzverbundwerkstoffe durch Verwendung anorganischer und organischer Nanopartikel (in German), Dissertation, *University of Erlangen-Nürnberg*, **2010**.